Medical Physics
The International Journal of Medical Physics Research and Practice

Evaluation of Al 2 O 3 : C optically stimulated luminescence (OSL) dosimeters for passive dosimetry of high-energy photon and electron beams in radiotherapy

E. G. Yukihara, G. Mardirossian, M. Mirzasadeghi, S. Guduru, and S. Ahmad

Citation: Medical Physics **35**, 260 (2008); doi: 10.1118/1.2816106
View online: http://dx.doi.org/10.1118/1.2816106
View Table of Contents: http://scitation.aip.org/content/aapm/journal/medphys/35/1?ver=pdfcov
Published by the American Association of Physicists in Medicine

Evaluation of Al_2O_3:C optically stimulated luminescence (OSL) dosimeters for passive dosimetry of high-energy photon and electron beams in radiotherapy

E. G. Yukihara[a)]
Department of Physics, Oklahoma State University, Stillwater, Oklahoma 74078

G. Mardirossian
Department of Radiation Oncology, Mount Sinai Comprehensive Cancer Center, Miami Beach, Florida 33140

M. Mirzasadeghi
Department of Radiation Oncology, University of Oklahoma Health Sciences Center, 825 Northeast 10th Street, OUPB 1430, Oklahoma City, Oklahoma 73104

S. Guduru
Department of Physics, Oklahoma State University, Stillwater, Oklahoma 74078

S. Ahmad
Department of Radiation Oncology, University of Oklahoma Health Sciences Center, 825 Northeast 10th Street, OUPB 1430, Oklahoma City, Oklahoma 73104

(Received 31 May 2007; revised 17 October 2007; accepted for publication 29 October 2007; published 21 December 2007)

This article investigates the performance of Al_2O_3:C optically stimulated luminescence dosimeters (OSLDs) for application in radiotherapy. Central-axis depth dose curves and optically stimulated luminescence (OSL) responses were obtained in a water phantom for 6 and 18 MV photons, and for 6, 9, 12, 16, and 20 MeV electron beams from a Varian 21EX linear accelerator. Single OSL measurements could be repeated with a precision of 0.7% (one standard deviation) and the differences between absorbed doses measured with OSLDs and an ionization chamber were within ±1% for photon beams. Similar results were obtained for electron beams in the low-gradient region after correction for a 1.9% photon-to-electron bias. The distance-to-agreement values were of the order of 0.5–1.0 mm for electrons in high dose gradient regions. Additional investigations also demonstrated that the OSL response dependence on dose rate, field size, and irradiation temperature is less than 1% in the conditions of the present study. Regarding the beam energy/quality dependence, the relative response of the OSLD for 18 MV was (0.51±0.48)% of the response for the 6 MV photon beam. The OSLD response for the electron beams relative to the 6 MV photon beam. The OSLD response for the electron beams relative to the 6 MV photon beam was in average 1.9% higher, but this result requires further confirmation. The relative response did not seem to vary with electron energy at d_{max} within the experimental uncertainties (0.5% in average) and, therefore, a fixed correction factor of 1.9% eliminated the energy dependence in our experimental conditions. © *2008 American Association of Physicists in Medicine*. [DOI: 10.1118/1.2816106]

Key words: optically stimulated luminescence, Al_2O_3:C, passive dosimetry, radiotherapy, mailed dosimetry, phantom measurements

I. INTRODUCTION

Solid-state passive dosimeters, mainly thermoluminescence dosimeters (TLDs), have been used to measure absorbed dose in radiotherapy for decades, offering advantages over many other dosimetry systems because of their small size, high sensitivity, measurement of integrated dose, lack of dependence on dose rate, possibility of multiple point measurements, and freedom from cables and high voltages.[1] Due to their properties and versatility, solid state passive dosimeters continue to play a role in radiotherapy using photons and electrons beams,[2,3] principally in mailed dosimetry intercomparisons and validation,[4–8] *in vivo* dosimetry, phantom measurements for quality assurance,[9,10] patient dose verification,[11,12] and investigations of the extra target and whole-body dose.[13,14]

Modern radiotherapy imposes new challenges for dosimetry systems in terms of absolute and spatial precision and accuracy. Treatments such as intensity modulated radiation therapy (IMRT) are capable of creating dose distributions with large dose gradients to conform better to the tumor, spare critical organs, and minimize the dose to healthy tissue.[15] These challenges incite investigations of new solid state passive dosimeters that can offer high precision, such as the optically stimulated luminescence dosimeter (OSLD).

Optically stimulated luminescence (OSL) is a technique that gained large acceptance in personal dosimetry during the last decade with the development of a high-sensitive dosim-

eter, carbon-doped aluminum oxide (Al_2O_3:C), and the introduction of the commercial Luxel™ dosimetry system.[16–19] Irradiated OSL dosimeters emit luminescence when exposed to light of appropriate wavelength. The physical process is similar to the TL process, with the exception that light, instead of heat, is used to stimulate the population of charges trapped at crystal defects created by exposure to ionizing radiation.[20]

Al_2O_3:C is the material of choice in OSL dosimetry due to its high sensitivity, linearity of response, relatively low effective atomic number (11.28),[21] and absence of fading.[19,22] Even though TL of Al_2O_3:C is already 40–60 times the sensitivity of LiF:Mg,Ti TLDs,[21] only the OSL technique takes full advantage of the material's high optical sensitivity and avoids problems associated with the thermal quenching of the luminescence.[16] The response is linear up to ~50–100 Gy, if only the main luminescence center (a broadband centered at 420 nm characteristic of *F*-centers in Al_2O_3:C) is detected.[18,23]

In spite of the similarities with the TL technique, the application of OSL in radiotherapy has been hampered by the lack of studies on the characteristics of Al_2O_3:C OSLDs for dosimetry of high-energy beams used in radiotherapy. However, this situation is starting to change.

Meeks *et al.* used OSLDs (Luxel™) to investigate the extra-target dose delivered to patients during intracranial and head and neck IMRT treatments. A preliminary test performed with OSLDs exposed to known doses between 0 and 0.264 Gy from a 10 MV linear accelerator photon beam revealed differences of up to 4.7% between the expected and measured doses.[24] Schembri and Heijmen also looked into using OSLDs in radiotherapy, having investigated fading, dosimeter response variations, dose rate dependence, linearity, beam quality dependence, field size and depth dependence, and response outside the radiation field for irradiations in a polystyrene phantom.[25] In both studies, the OSLDs were sent to Landauer Inc. for readout. The results from Schembri and Heijmen are very helpful to understand the performance of OSLDs with commercially available services. Their results showed a dependence on dose rates smaller than 1%, linear response below 2 Gy with onset of supralinearity for higher doses, differences between photon and electron beam responses equal to 3.7%, and a difference of 4.1% between 6 and 18 MV photon beams. The deviations due to field size were within ±2.5%.[25]

We recently introduced an OSL readout methodology that resulted in dose estimates with uncertainty for a single readout (experimental standard deviation) of ~0.7%, which represents a considerable improvement over commercially available systems.[26] This reproducibility is given by the experimental standard deviation of the OSL response of 50 dosimeters irradiated with a dose of 0.665 Gy from a 6 MV photon beam with a SSD of 100 cm at a 10 cm depth in water phantom. A preliminary depth dose curve obtained in water phantom using the 6 MV photon beam showed good agreement between the OSL values and the Varian linear accelerator commissioning data, the maximum difference observed being 1.1%. These results were obtained using an automated reader[27] without control of mass of the dosimeters and equipment sensitivity, and without correction for fading or time elapsed since irradiation. The reproducibility previously mentioned can be compared with results from Izewska *et al.* showing a standard deviation of 0.8% for an average of 8 TLD readings,[6] and results from Kirby *et al.* showing a standard deviation of 1.4% for single TLD readouts.[7] Using commercial OSLD readout, Schembri and Heijmen obtained distributions with standard deviation between 1.0 and 3.2% in six measurement sessions.[25]

The results obtained with the proposed methodology motivated the present investigations on the performance of Al_2O_3:C OSLDs for other photon and electron beams. These investigations are also motivated by the increased use of OSL in medical dosimetry using commercially available systems,[28–34] parallel advances in the development of *in vivo* real-time dosimetry systems for radiotherapy that use Al_2O_3:C probes connected to a reader via optical fiber cables,[35–41] and the consequent need for an independent characterization of Al_2O_3:C.

The present work investigates the performance of Al_2O_3:C OSLDs using a variety of photon and electron beam energies at different depths in a water phantom under different conditions of dose rate, temperature, and field size. The objective is to determine the accuracy and precision of the OSL measurements using the new methodology, as compared to an ionization chamber used for calibration of the linear accelerators. We also intend to investigate the dependence of the OSLDs on beam energy, dose rate, field size, and irradiation temperature within a radiation therapy operational setup.

II. MATERIALS AND METHODS

II.A. Dosimeters

The OSLDs used in this study are 7 mm in diameter and 0.3 mm thick and consist of polyester film containing Al_2O_3:C powder (grain sizes $<105\ \mu$m). The dosimeters were prepared from new Luxel™ dosimeters (Landauer Inc.)[19] using a hole puncher. No strict control in the dosimeter mass was necessary; the OSL readout procedure used in this study was shown to take into account any variation in the mass or sensitivity of the dosimeters.[26] Before irradiation, the dosimeters were illuminated with yellow light from a halogen lamp filtered by a yellow glass Kopp 3-69 filter to eliminate any signal accumulated during storage.

For the irradiations, the dosimeters were packaged with black tape (34.0 mg/cm^2 on each side of the package) to prevent exposure to light during irradiation, transportation, and handling, with each package containing three to five dosimeters placed side by side. The total thickness of the packages was 0.9 mm. Packages containing only one dosimeter were also prepared to test whether the number of dosimeters in the package influences the results, but no difference was observed for a 10 cm × 10 cm field size within the experi-

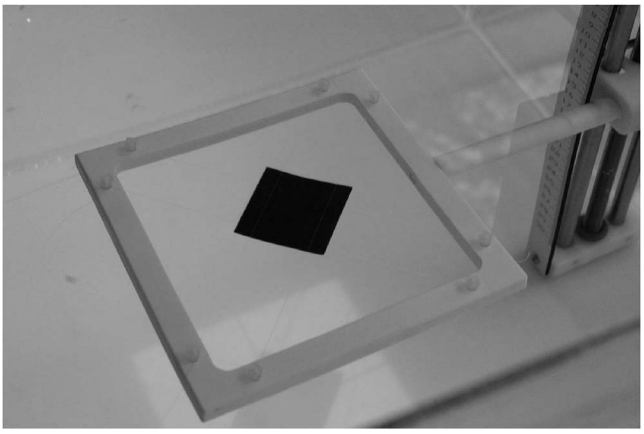

FIG. 1. Dosimeter holder containing one OSLD package inside the water phantom. The dosimeter holder was designed for these experiments and consisted of water equivalent plastic containing thin nylon strings across the diagonals to support the packages.

mental uncertainties. In these experiments the dosimeters were not reused and the possibility of reusing them was not investigated at this time.

II.B. Irradiations

Irradiations with photon and electron beams were carried out using a Varian 21 EX linear accelerator at the Department of Radiation Oncology, University of Oklahoma Health Sciences Center. The irradiations were performed inside a 40 cm × 45 cm × 38 cm water phantom from Radiation Products Design Inc. (model 691-015), filled with water to a depth of 30 cm. The accelerator was calibrated with a 10 cm × 10 cm field size source-to-surface distance (SSD) setup using TG-51 calibration protocol at a depth of 10 cm.[42]

For the irradiations, a holder specially designed for these experiments supported each dosimeter package inside the water phantom. The holder consists of a 1 cm thick 12 cm × 12 cm square frame, machined from a slab of water equivalent plastic (Plastic Water™, Computerized Imaging Reference Systems, Inc.), which is optimized to simulate water at energies between 0.5 and 100 MeV. The frame contains four 0.2 mm diameter nylon strings across the diagonals to hold the dosimeter package from both sides (Fig. 1). The holder was connected to the positioning system that controls the vertical position of the holder via a remote digital motor drive controller, thus allowing the precise positioning of the dosimeter packages inside the water phantom.

Before each irradiation sequence, the SSD was carefully monitored with the optical distance indicator (ODI). The dosimeter in the holder was then positioned at the water surface and aligned with the central axis of the linear accelerator. At this position, the digital indicator of the motor drive controller was reset. The dosimeter was then moved to the desired depth using the calibrated motor drive controller. To avoid possible backlash positioning errors, the procedure was carried out only in the downward direction.

Every time the holder was brought to the surface, the procedure previously described was repeated to eliminate errors due to backlash. In addition, even during the irradiation sequence the SSD was checked with the ODI to ensure that no significant water was lost due to evaporation or the frequent change of dosimeters.

The irradiations were performed with a 10 cm × 10 cm field size and dose rate of 400 MU/min (4 Gy/min at d_{max}), except when mentioned otherwise. The temperature of the water was monitored using a mercury thermometer.

Additionally, a 40 mCi $^{90}Sr/^{90}Y$ beta source integrated in the Risø TL/OSL-DA-15 reader was also used to deliver a reference dose to the OSLDs. The source is calibrated in ^{60}Co gamma dose to water.

II.C. Ionization chamber measurements

In this study, the OSL data was compared to ionization chamber measurements. The central-axis percent depth dose (PDD) curves for photons and electrons were obtained during the annual routine calibration using two Scanditronix/Wellhofer CC13 ionization chambers, a 3D Scanditronix/Wellhofer Blue Water phantom tank, and a Scanditronix/Wellhofer CU500E controller unit, with OmniPro Accept software. For the investigation on the energy dependence of OSLDs, the irradiations were carried out on the same day of the monthly routine calibration. The monthly calibration was performed using an Exradin Farmer A12 ionization chamber and Standard Imaging Max 4000 electrometer. The annual and monthly routine calibrations were carried out according to the TG-51 calibration protocol.[42]

II.D. OSL readout equipment

The OSL measurements were carried out using an automated Risø TL/OSL-DA- 15 reader[27] (Risø National Laboratory, Denmark) equipped with green LEDs for light stimulation (525 nm, ~10 mW/cm^2), and a photomultiplier tube (PMT), model 9235QB (Electron Tubes Inc.), for detection of the luminescence from the dosimeters. Hoya U-340 filters (7.5 mm thickness; transmission between 290–390 nm) were used in front of the PMT to block the stimulation light, while allowing the OSL signal from the dosimeter to reach the PMT. An extra 2 mm Schott glass filter WG-360 was used to remove the UV component of the emission spectrum of $Al_2O_3:C$, which shows an undesirable time-dependent increase in intensity following irradiation[23]. In these conditions, only the tail of the main luminescence band of $Al_2O_3:C$ is detected. This does not represent a problem, since the material is sensitive enough to allow the estimation of doses of the order of 0.1 mGy with the current equipment. However, since the doses of interest in this case are 3–5 orders of magnitude higher, an additional aperture of 24 mm in diameter was used in front of the PMT to reduce the intensity of the OSL signal, avoiding PMT saturation and nonlinearity of the PMT response.

II.E. OSL readout procedure

For each dosimeter, the readout procedure consisted of the following steps:

(i) The irradiated dosimeter was stimulated for 600 s to record the OSL decay curve, from which the total OSL signal S, due to the dose from the linear accelerator, was calculated.

(ii) The dosimeter was then irradiated in a laboratory with a reference dose of approximately 0.96 Gy using the $^{90}Sr/^{90}Y$ source. (Note: the value of the dose used in this step is not used in the calculations; it only needs to be the same and reproducible throughout the procedure, including the determination of the calibration curve.)

(iii) The dosimeter was again stimulated during 600 s to record the OSL decay curve, from which the total OSL signal S_R, this time due to the reference dose, was calculated. The ratio S/S_R was then converted to an absorbed dose using a calibration curve of S/S_R versus the dose previously obtained with a separate set of dosimeters.

Steps (ii) and (iii) were used to eliminate the influence of the dosimeter mass, sensitivity, and reader sensitivity.[26] In steps (i) and (iii), the PMT signal during the last 10 s of stimulation is considered as a background and subtracted from the OSL curves before calculation of S and S_R.

A total of 24 dosimeters can be placed in the Risø reader tray and loaded into the reader at one time. The process of loading the dosimeters takes approximately 15 min and was performed under subtle light (e.g., under 25 W red bulb light). The reader then carried out the OSL readout and irradiation sequence automatically. Approximately ~20 min is required for each dosimeter to be completely analyzed, since the OSL readouts in steps (i) and (iii) take 10 min each. The duration of the OSL readout is determined by the limitation in the maximum power of the LEDs in the current equipment (~10 mW/cm^2). Higher stimulation intensities can read the OSL signal faster,[20] reducing the readout time without loss of quality in the results. The readout time can also be improved by sampling the OSL signal for a shorter period, 1 s for example, as usual in commercial systems. However, this may introduce a dependence of the OSL on the total stimulation energy delivered to the dosimeters that we wanted to avoid in this study.

The calibration curve S/S_R versus the absorbed dose was determined using a set of dosimeters irradiated with various doses of a 6 MV photon beam, 10 cm × 10 cm field size, SSD = 100 cm, at 10 cm depth in the water phantom.

Except when mentioned otherwise, the standard deviations presented in this study are the experimental standard deviation (dispersion of individual results), therefore indicating the uncertainty associated with a single OSL measurement.[43]

III. RESULTS

III.A. OSL dose response and calibration curve

The dose response of the OSLDs was determined using a 6 MV photon beam for doses between 6.65 cGy and 6.65 Gy, corresponding to irradiations from 10 to 1000 MU at a 10 cm depth in water. Each dosimeter package contained three dosimeters. The OSL readouts were carried out according to the procedure described in Sec. II E, from which both the signal S (due to the linear accelerator irradiation) and the signal S_R (due to the reference dose) are obtained.

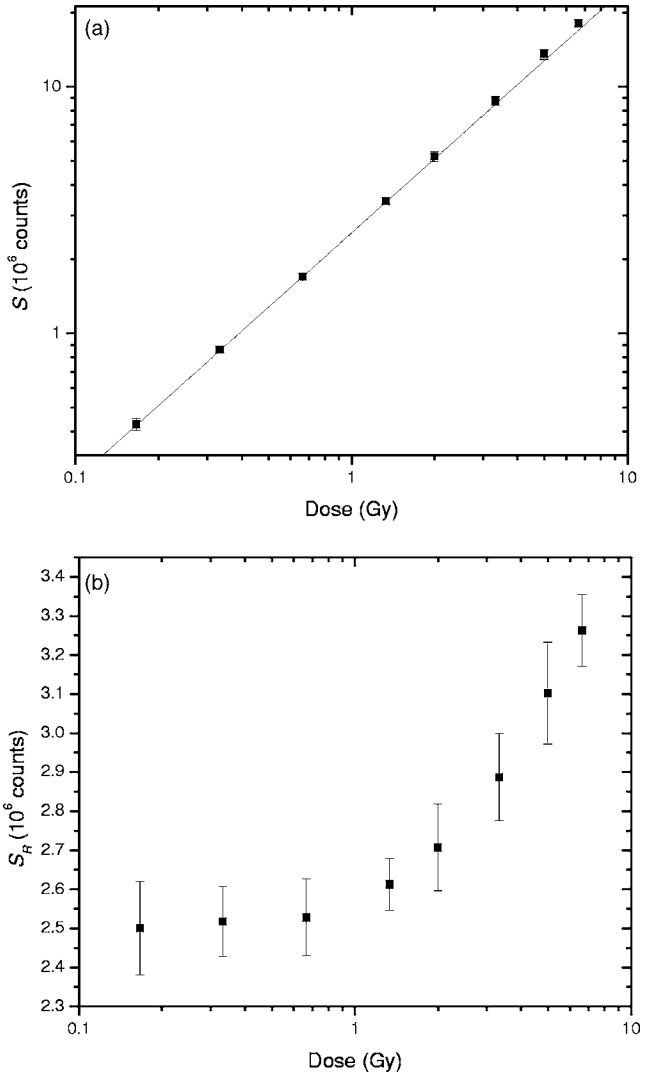

FIG. 2. (a) Total OSL signal S recorded after irradiation with different doses from a 6 MV photon beam. The line represents the linear response in this scale. (b) Total OSL signal S_R after the same dosimeters used in (a) are irradiated with a $^{90}Sr/^{90}Y$ reference, as a function of the dose given by the 6 MV photon beam from the linear accelerator. The data points represent the mean value of five dosimeters and the error bars represent the experimental standard deviation.

Figure 2(a) shows that the signal S resulting from the 6 MV photon irradiation is linear over the range of doses investigated, with a possible small supralinearity for doses above ~5 Gy. The experimental standard deviation of S, indicated by the error bars, is relatively large (4.1% on average) because of variations in dosimeter mass and sensitivity.

The irradiations in the linear accelerator cause an increase in the dosimeter's sensitivity due to filling of deep traps that are not emptied by the optical stimulation.[44] The effect of the sensitization caused by the previous irradiation on S_R is illustrated in Fig. 2(b), which shows the signal S_R as a function

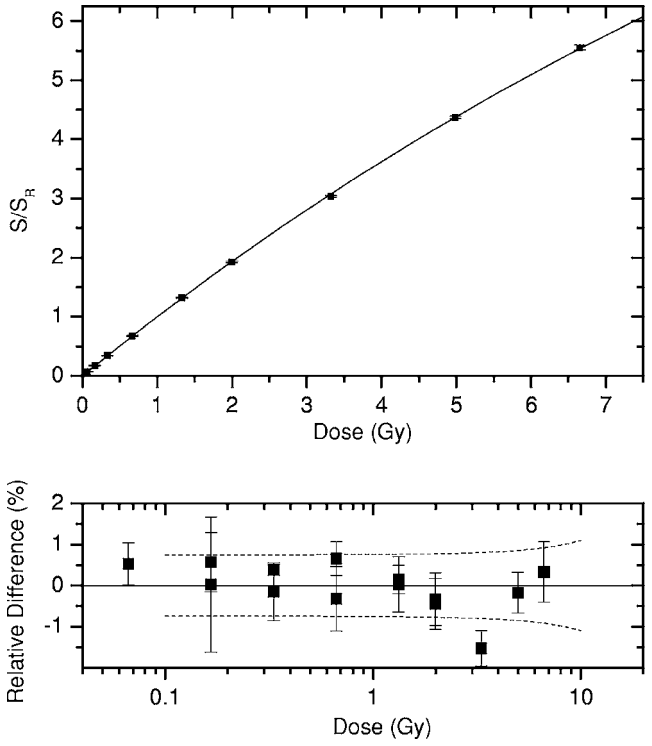

FIG. 3. (a) Ratio S/S_R between the OSL signal S after irradiation in the accelerator with the indicated dose, and the OSL signal S_R after subsequent irradiation with a reference dose. (b) Relative difference between the OSL data and the fitted saturating exponential [Eq. (1)] with parameters $a=15.11\pm0.20$ and $b=(0.0686\pm0.0011)$ Gy^{-1}. The dashed lines are the relative standard deviation of the dose σ_D as a function of dose, calculated using Eq. (2) and the above fitted values for a and b, as well as a covariance of -2.12×10^{-4} Gy^{-1} obtained from the fitting procedure. The data points represent the mean value of five dosimeters and the error bars represent the experimental standard deviation. [Note that the error bars are smaller than the size of the symbols in (a).] Duplicate irradiations were carried out for some doses.

of the dose previously delivered by the linear accelerator. The experimental standard deviation of S_R is 3.7% on average. The signal S_R increases as much as 30% as the dose previously delivered by the linear accelerator is increased from 0.3 to 6.6 Gy. Consequently, S/S_R is not linear with dose.

Figure 3(a) shows the ratio S/S_R plotted as a function of the dose delivered by the linear accelerator. The error bars indicate that the normalized OSL signal is S/S_R is characterized by a smaller dispersion than the values S, revealing the advantage of using S/S_R for the analyses. The average relative experimental standard deviation of S/S_R is 0.63%, in agreement with our previous investigation.[26]

We found that the dose response of S/S_R from Fig. 3(a) can be described by a saturating exponential [Eq. (1)] of the form

$$\frac{S}{S_R}=a(1-e^{-bD}). \tag{1}$$

with parameters $a=15.11\pm0.20$ and $b=(0.0686\pm0.0011)$ Gy^{-1}. The relative difference between S/S_R and the fitted curve is plotted in Fig. 3(b). With one exception, the errors are within ±1%. Since the S/S_R ratio cancels sensitivity changes in the equipment, the same calibration curve was used regardless of the day of readout. The ratio S/S_R also cancels variations in the sensitivity between different dosimeters within the same batch. (The possibility of using the same calibration curve for different batches was not tested, although it may represent an advantage of this procedure, provided that the material properties other than the sensitivity do not change significantly from batch to batch.)

III.B. Uncertainties associated with the calibration curve

To determine the uncertainty associated with the use of the calibration curve shown in Fig. 3 and represented by Eq. (1), the standard deviation of the estimated doses was calculated based on Eq. (1), the standard deviation of the fitted parameters a and b, the covariance between the fitted parameter $\mathrm{cov}(a,b)$, and the uncertainty σ_x in the variable $x=S/S_R$ using the following equation:[43]

$$\sigma_D^2=\left(\frac{\partial D}{\partial a}\right)^2\sigma_a^2+\left(\frac{\partial D}{\partial b}\right)^2\sigma_b^2+2\left(\frac{\partial D}{\partial a}\right)\left(\frac{\partial D}{\partial b}\right)\mathrm{cov}(a,b)+\left(\frac{\partial D}{\partial x}\right)^2\sigma_x^2, \tag{2}$$

where $D=D(x)$ is the inverse function of Eq. (1). The parameters a and b, respective uncertainties σ_a and σ_b, and the covariance term $\mathrm{cov}(a,b)$ between a and b were obtained from the fit to the data in Fig. 3 (see caption in Fig. 3). The relative standard deviation σ_x/x associated with S/S_R was taken to be 0.63%.[26]

In Fig. 3(b), the curves corresponding to $\pm\sigma_D$ [Eq. (2)] are plotted as a function of dose [Fig. 3(b), dashed lines]. These curves show that the uncertainty in the absorbed dose measurements (using a single OSL dosimeter) remains approximately constant at 0.74% in the low dose range, increasing to a maximum of 1.1% at 10 Gy.

III.C. Depth dose curve for photons

Depth dose curves were measured for 6 and 18 MV photons using OSL packages containing either five dosimeters or one dosimeter. The absorbed doses were obtained from the S/S_R values of the irradiated dosimeters using the calibration curve shown in Fig. 3(a). The OSL doses obtained were normalized to the maximum dose to obtain the PDD values. The PDD curves thus obtained were compared with the ionization chamber reference data of the linear accelerator, as shown in Fig. 4.

First of all, Fig. 4 shows that no difference was observed between packages containing five dosimeters or one dosimeter. If we exclude the region of high dose gradients in the build-up region (depth $d<10$ mm for 6 MV and $d<15$ mm for 18 MV photons), the difference between the absorbed dose for the packages with one dosimeter and five

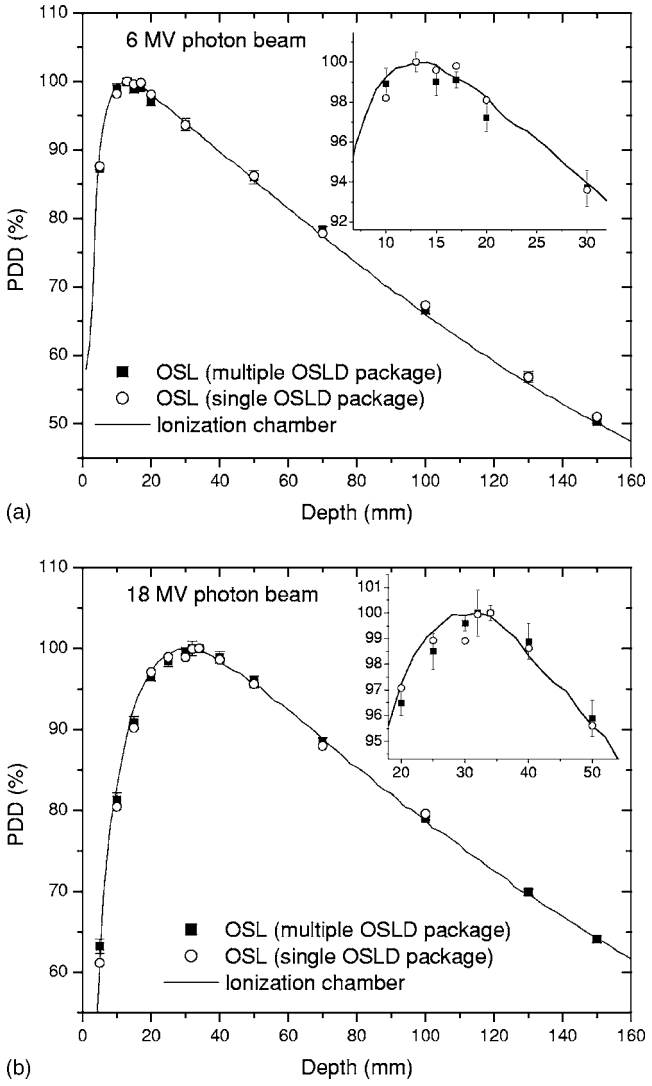

FIG. 4. Central-axis percent depth dose (PDD) curves for (a) 6 MV and (b) 18 MV photon beams obtained using OSLDs and the ionization chamber. In both cases, data obtained using packages containing either five dosimeters or one dosimeter are presented. The data points for packages containing multiple OSLDs are the mean value of the dosimeters, and the error bars (barely visible) represent the experimental standard deviation. The insets show the same data in the region around d_{max}.

dosimeters is $(-0.17\pm0.13)\%$. This is consistent with the assertion that both dosimeter packages give the same result within $\pm2\sigma$.

The absolute agreement between the OSL and the ionization chamber data is also good in both cases. Excluding again the high dose gradient regions, the distribution of relative errors for both photon energies had a mean value of 0.1% and a standard deviation of 0.7%. (In this study we adopt the definition of relative error as the measurement minus the true value of the measurand, divided by the true value of the measurand,[43] where the "true value" is considered to be the ionization chamber value.) This means that in ~63% of the cases, the OSL data is within −0.6% and +0.8% from the ionization chamber values. The maximum relative errors were 1.7% for 6 MV photon beam (d =130 mm) and 0.7% for 18 MV photon beam (d=20 mm).

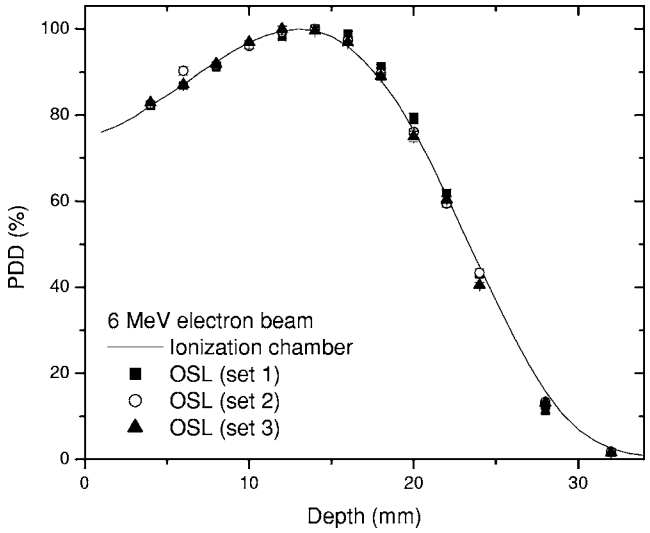

FIG. 5. Central-axis percent depth dose (PDD) curves for 6 MeV electron beam obtained using OSLDs and the ionization chamber. The graph presents three data sets obtained in subsequent sequences of irradiations. The data points are the mean value of the dosimeters for each package, and the error bars (barely visible) represent the experimental standard deviation.

The average experimental standard deviation of the values from the 5 dosimeter package was 0.7%, in agreement with our previously reported uncertainties.[26]

As can be observed in Fig. 4, the OSL data also agrees well with the ionization chamber values in the build-up region.

III.D. Uncertainty associated with dosimeter positioning

The precision for dosimeter positioning is more critical in the determination of the depth-dose curves for electron beams compared to photon beams because of the presence of large dose gradients. To investigate the reproducibility in the determination of the PDD curves for a 6 MeV electron beam, we repeated the whole irradiation sequence three times and compared the depth dose curves obtained.

The PDD values obtained for the irradiation sequences are shown in Fig. 5. The distribution of relative errors in the region of low dose gradients (depth d in the range 4 mm $\leqslant d \leqslant$ 16 mm) had a mean value of 0.1% and a standard deviation of 1.0%. (This result does not include the outlier in set 2 corresponding to d=6 mm, which, given the precision of the measurements, we attribute to a mistake in the positioning of the dosimeter during irradiation.) Again, this implies that in ~63% of the cases, the OSL data are within −0.9% and 1.1% from the ionization chamber data. In the region of high dose gradients ($d \geqslant 18$ mm) the mean distance-to-agreement (DTA) value is 0.2 mm with a standard deviation of 0.5 mm. These values were calculated considering all three data sets.

III.E. Depth dose curves for electrons

The depth dose curves were also measured for 9, 12, 16, and 20 MeV electron beams using the same procedure em-

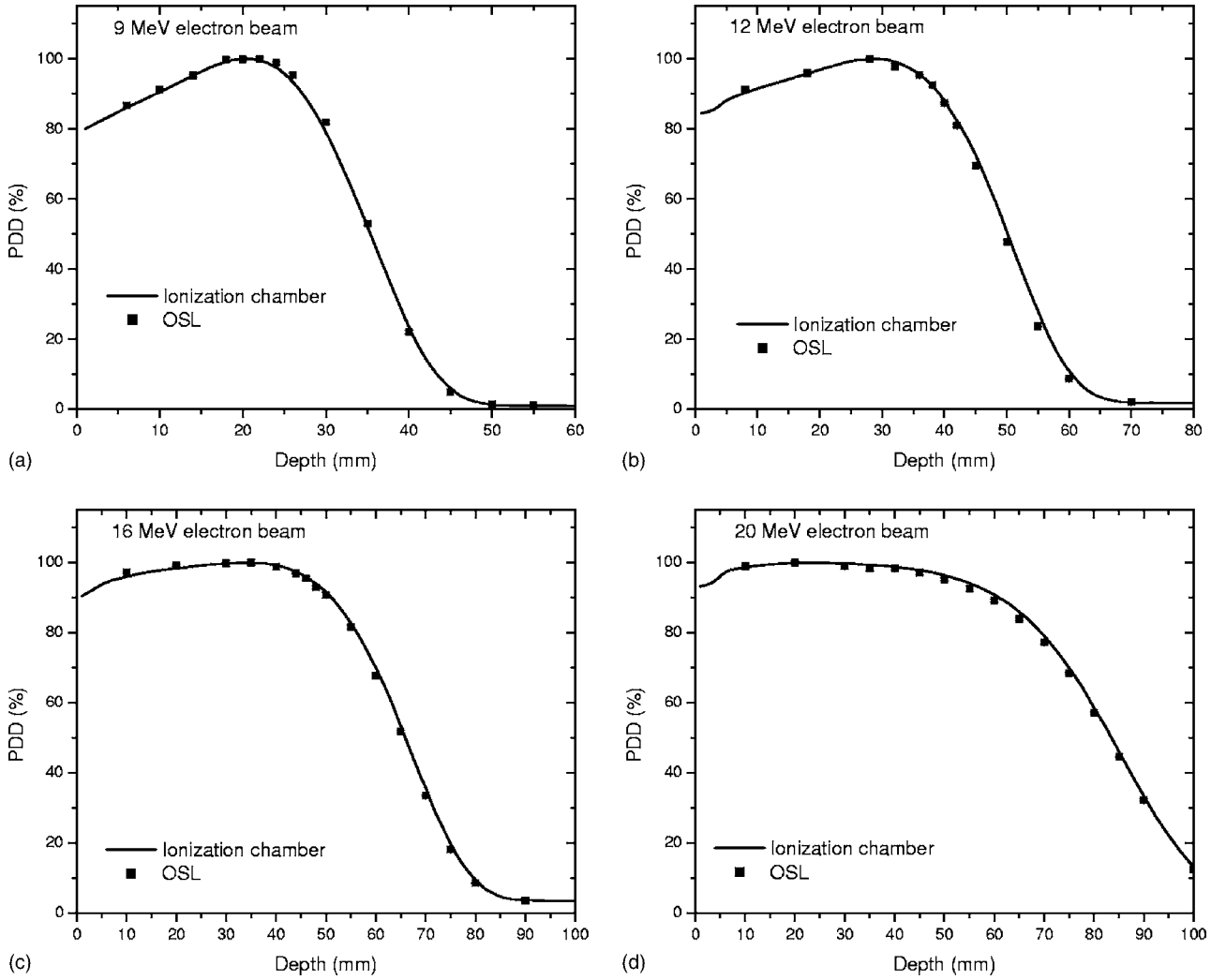

FIG. 6. Central-axis percent depth dose (PDD) curves for (a) 9 MeV, (b) 12 MeV, (c) 16 MeV, and (d) 20 MeV electron beams obtained using OSLDs and the ionization chamber. The data points are the mean value of the dosimeters for each package, and the error bars (barely visible) represent the experimental standard deviation.

ployed in the previous sections. In all cases we used dosimeter packages containing five dosimeters. The OSL doses were obtained from the S/S_R for each dosimeter using the 6 MV photon calibration curve shown in Fig. 3. The OSL doses were then normalized to the maximum dose to obtain the PDD values.

The central-axis depth dose curves obtained using OSLDs and ionization chamber are compared in Fig. 6. In the region of low dose gradients (9 MeV: $d \leqslant 24$ mm; 12 MeV: $d \leqslant 38$ mm; 16 MeV: $d \leqslant 50$ mm; 20 MeV: $d \leqslant 60$ mm), the mean relative error is 0.1% with a standard deviation of 0.8%. In the region of large dose gradients (9 MeV: 26 mm $\leqslant d \leqslant 45$ mm; 12 MeV: 40 mm $\leqslant d \leqslant 60$ mm; 16 MeV: 55 mm $\leqslant d \leqslant 80$ mm; 20 MeV: 65 mm $\leqslant d \leqslant 90$ mm), the mean DTA is 0.52 mm with a standard deviation of 0.55 mm.

III.F. Energy dependence

To determine the energy dependence of Al_2O_3:C for photon and electron beams, OSLDs were irradiated with 100 MU at d_{max} with the 6 and 18 MV photon beams and with the 6, 9, 12, 16, and 20 MeV electron beams. The routine monthly calibration was performed in the same day, before the OSL irradiations. Each OSL package consisted of five dosimeters, from which the absorbed doses were calculated using the calibration curve obtained using 6 MV photon irradiation shown in Fig. 3(a).

The response of the OSLDs relative to the 6 MV photon beam is shown in Fig. 7. The relative response was calculated dividing the OSLD response by the machine calibration factor obtained with the ionization chamber during the monthly calibration. The results were then normalized to the relative response for the 6 MV photon beam to eliminate variations in the machine output between the day of the present measurements and the day in which the OSL calibration curve was obtained, therefore isolating only effects due to energy of the beam. The error bars in this case are the combined standard deviation after appropriate uncertainty propagation.[43]

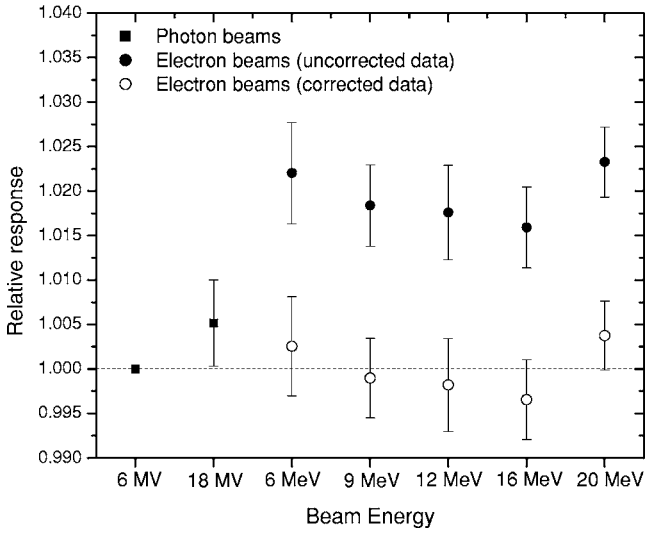

FIG. 7. Relative response of OSLDs for photon and electron beams of various energies relative to the response for 6 MV photon beam. The uncorrected data for electrons shows an average over-response of 1.9%. The corrected electron data were obtained dividing all uncorrected values for electrons by a fixed value of 1.019.

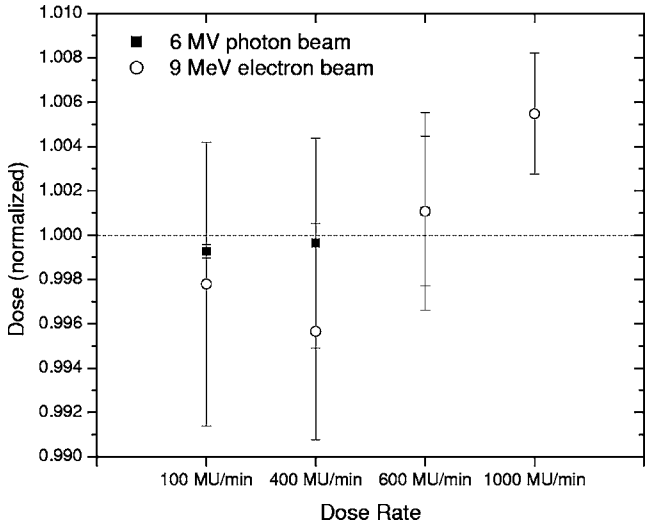

FIG. 8. Dose rate dependence of the OSL response S/S_R for 6 MV photon beam and 9 MeV electron beans. The detectors were irradiated with 200 MU at a 10 cm depth in the case of the 6 MV photon beam, and at a 2 cm depth in the case of the 9 MeV electron beam. The data points are the average dose of five OSLDs, normalized to the mean value of each respective data set, and the error bars represent the experimental standard deviation.

For the photon beams, the difference between the 18 and 6 MV photon beams is $(0.51 \pm 0.48)\%$, therefore identical within a 95% confidence interval (2σ). In the case of the electron beams, the response of the OSLDs (Fig. 7, "uncorrected data") photon beam is on average 1.9% higher than the response to the 6 MV photon beam. However, if the data are corrected for this overresponse (Fig. 7, "corrected data"), the relative response does not seem to depend on electron energy within the experimental uncertainties.

III.G. Effect of dose rate, field size, and irradiation temperature

Additional measurements were carried out to verify the effect of dose rate, field size, and irradiation temperature on the OSLDs. It must be mentioned that these experiments were carried out with an earlier type of sample holder that did not provide the same support for the dosimeters as the new sample holder described in Sec. II B. However, the results were satisfactory and we did not consider it necessary to repeat the measurements with the new holder.

The effect of dose rate variation was investigated irradiating the OSLD packages, each containing three dosimeters, with 200 MU at a 10 cm depth in water with dose rates of 100, 400, and 600 MU/min from a 6 MV photon beam, and with 200 MU at a 2 cm depth in water with dose rates between 100 and 1000 MU/min from a 9 MeV electron beam. It should be pointed out that this test only investigates the dependence of OSL on the linear accelerator dose rate setting and not the actual dose rate delivered to the dosimeter, given that the dose by the linear accelerator is delivered in pulses of variable pulse-repetition frequency.

The absorbed dose values obtained for the 6 MV photon beam and the 9 MeV electron beam at different dose rates are shown in Fig. 8. The variation in the OSL response in all cases is smaller than ±1%.

To investigate the effect of the field size, the dosimeter packages were irradiated with 200 MU from a 6 MV photon beam at a 10 cm depth in water using field sizes ranging from 5 cm × 5 cm to 30 cm × 30 cm. The doses determined using OSLDs and the ionization chamber for different field sizes are compared in Fig. 9. The maximum discrepancy ob-

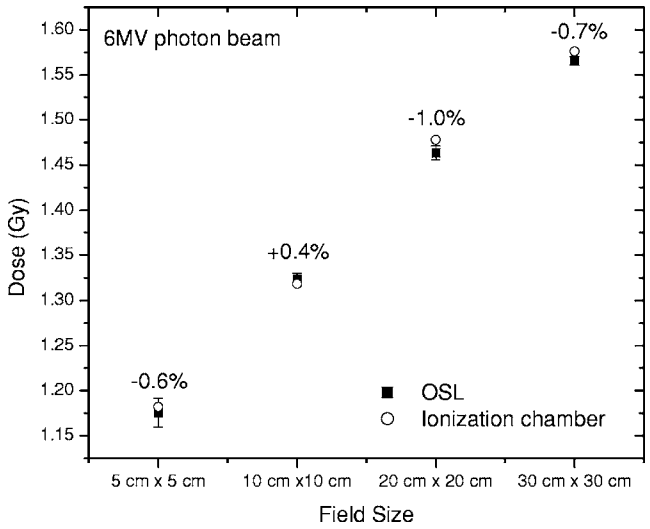

FIG. 9. Doses obtained using OSLDs and ionization chambers for different field sizes. In all cases the irradiations were carried out with 6 MV photon beam, 200 MU, and at 10 cm depth in water. The data points are the average of 5 OSLDs and the error bars represent the experimental standard deviation.

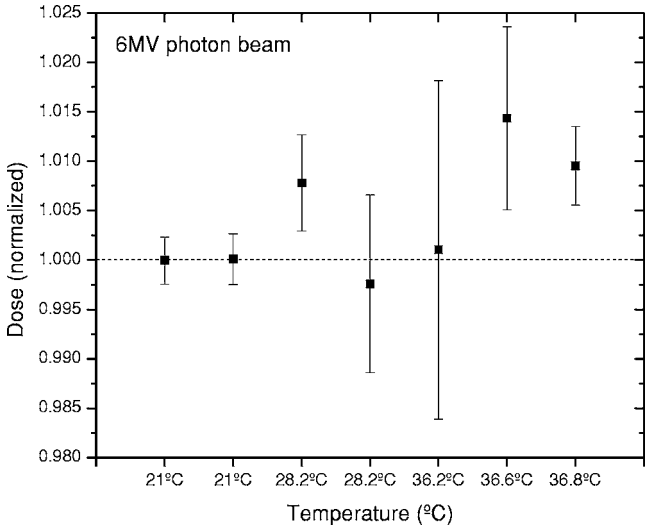

FIG. 10. Doses obtained using OSLDs at different temperatures, for irradiation with 100 MU and 10 cm depth in water. The data points are the average of 5 OSLDs, normalized to the mean value of the room temperature points (21 °C), and the error bars represent the experimental standard deviation.

served was 1%.

Finally, the effect of irradiation temperature was investigated irradiating the OSLD packages in water at different temperatures. The water temperature was raised from ~21 °C up to ~36 °C by gradually replacing the water in the tank with hot tap water. The irradiations were carried out using a 6 MV photon beam, with a 100 MU irradiation, at a depth of 10 cm. The results on the temperature dependence of the OSL signal presented in Fig. 10 show variations within ±1%. This result is in agreement with earlier investigations on an optical fiber dosimetry system that uses Al_2O_3:C as a probe.[35,45] Edmund *et al.*[46] observed a variation of ~1% in the OSL signal of Al_2O_3:C crystals as the temperature is increased from ~20 °C to ~40 °C when the integration time is long (600 s of stimulation).

IV. DISCUSSION AND CONCLUSIONS

The results obtained in this work show that, apart from errors introduced by positioning of the samples that will naturally affect the results in regions of high dose gradient, the OSL technique consistently gives results that are within ±1% of the values obtained with the ionization chamber. In regions of high dose gradient for electron beams, the DTA is of the order of 0.5–1.0 mm. Dose rate, field size, and temperature did not affect the OSL results by more than 1%.

Regarding the beam energy/quality dependence for photon beams, the difference between the OSL response at 18 MV and the 6 MV photon beams is (0.51±0.48)%. This result agrees with energy response investigation on Al_2O_3:C optical fibers by Aznar.[35] Also, Mobit *et al.* predicted a difference of only 1.0% between 15 and 6 MV photon beams using Monte Carlo calculations, although for a significantly larger single crystal (2.85 mm diameter by 1 mm thickness).[47] Nevertheless, it should be pointed out that Schembri and Heijman observed a discrepancy of 3.7% for OSLDs irradiated in a polystyrene phantom irradiated with 18 and 6 MV photon beams, pointing out the need for more detailed investigations on this relatively new material with particular attention to the experimental conditions.[25]

For electron beams, an overresponse of 1.9% was observed for the OSLDs when compared to the 6 MV photon beam. At this point, the 1.9% overresponse cannot be attributed unequivocally to the OSLDs, since differences of the order of 1.8% are observed depending on the model of cylindrical ionization chamber used[48] or protocol adopted (TG-21 versus TG-51).[49,50] The results are also in contrast with data from Schembri and Heijmen using polystyrene phantom, which shows an underresponse for electrons of 3.7% compared to photon beams, demonstrating the need for more investigations on the electron response of Al_2O_3:C. Nevertheless, the OSLD response at d_{max} does not seem to depend on electron energy within the experimental uncertainties (0.5% on average) and, therefore, a fixed correction factor of 1.9% was sufficient to eliminate the difference between the electron data and the 6 MV photon data.

In spite of the promising results obtained in this study, there are disadvantages to be considered in OSL dosimetry. The first one is the intrinsic optical sensitivity of the dosimeters, which requires the OSLDs to be protected from light after exposure to radiation. The second one is the availability and cost of OSL readers capable of automatically performing the procedure adopted in the present study. We believe the latter is related to the fact that OSL is a relatively new technique; the technical gap may disappear as OSL applications spread into fields other than personal dosimetry, in which OSL dosimetry is already established. Regarding the optical sensitivity, the advantages already introduced by OSL and future developments in equipment may balance or even exceed the disadvantage of having to protect the OSLDs from light, making it an attractive alternative to TLDs in applications such as mailed dosimetry and phantom measurements.

ACKNOWLEDGMENTS

The authors would like to thank Dr. Elisabeth M. Yoshimura for suggestions on the manuscript, Landauer Inc. for the Luxel™ OSLDs used in this study, and Mike Lucas from the OSU Physics and Chemistry Instrument shop for the construction of the dosimeter holder. This work was a collaborative effort of all of the authors and the data collected were used as partial fulfillment of two Master of Science projects by Mirzasadeghi and Guduru. The project was supported by start-up funds provided by Oklahoma State University.

[a]Author to whom all correspondence should be addressed. Electronic mail: eduardo.yukihara@okstate.edu

[1]T. Kron, "Applications of thermoluminescence dosimetry in medicine," Radiat. Prot. Dosim. **85**, 333–340 (1999).
[2]K. R. Hogstrom and P. R. Almond, "Review of electron beam therapy physics," Phys. Med. Biol. **51**, R455–R489 (2006).
[3]F. d'Errico, "Dosimetric issues in radiation protection of radiotherapy patients," Radiat. Prot. Dosim. **118**, 205–212 (2006).
[4]D. Kroutilíková, J. Novotný, and L. Judas, "Thermoluminescent dosimeters (TLD) quality assurance network in Czech Republic," Radiother. Oncol. **66**, 235–244 (2003).

[5]P. Cadman *et al.*, "Dosimetric considerations for validation of a sequential IMRT process with a commercial treatment panning system," Phys. Med. Biol. **47**, 3001–3010 (2002).
[6]J. Izewska, P. Bera, and S. Vatnitsky, "IEAE/WHO TLD postal dose audit service and high precision measurements for radiotherapy level dosimetry," Radiat. Prot. Dosim. **101**, 387–392 (2002).
[7]T. H. Kirby, W. F. Hanson, and D. A. Johnston, "Uncertainty analysis of absorbed dose calculations from thermoluminescence dosimeters," Med. Phys. **19**, 1427–1433 (1992).
[8]S. Derreumaux *et al.*, "A European quality assurance network for radiotherapy: dose measurement procedure," Phys. Med. Biol. **40**, 1191–1208 (1995).
[9]A. Molineu *et al.*, "Design and implementation of an anthropomorphic quality assurance phantom for intensity-modulated radiation therapy for the radiation therapy oncology group," Int. J. Radiat. Oncol., Biol., Phys. **63**, 577–583 (2005).
[10]G. S. Ibbott, A. Molineu, and D. S. Followill, "Independent evaluations of IMRT through the use of an anthropomorphic phantom," Technol. Cancer Res. Treat. **5**, 481–487 (2006).
[11]D. Verellen *et al.*, "Initial experience with intensity-modulated conformal radiation therapy for treatment of the head and neck region," Int. J. Radiat. Oncol., Biol., Phys. **39**, 99–114 (1997).
[12]D. A. Low *et al.*, "Quality assurance of serial tomotherapy for head and neck patient treatments," Int. J. Radiat. Oncol., Biol., Phys. **42**, 681–692 (1998).
[13]S. Mutic and D. A. Low, "Whole-body dose from tomotherapy delivery," Int. J. Radiat. Oncol., Biol., Phys. **42**, 229–232 (1998).
[14]M. Mazonakis *et al.*, "Brain radiotherapy during pregnancy: an analysis of conceptus dose using anthropomorphic phantoms," Br. J. Radiol. **72**, 274–278 (1999).
[15]T. Bortfeld, "IMRT: a review and preview," Phys. Med. Biol. **2006**, R363–R379 (2006).
[16]M. S. Akselrod *et al.*, "Optically stimulated luminescence of Al_2O_3," Radiat. Meas. **29**, 391–399 (1998).
[17]S. W. S. McKeever and M. S. Akselrod, "Radiation dosimetry using pulsed optically stimulated luminescence of Al_2O_3:C," Radiat. Prot. Dosim. **84**, 317–320 (1999).
[18]M. S. Akselrod and S. W. S. McKeever, "A radiation dosimetry method using pulsed optically stimulated luminescence," Radiat. Prot. Dosim. **81**, 167–176 (1999).
[19]L. Bøtter–Jensen, S. W. S. McKeever, and A. G. Wintle, *Optically Stimulated Luminescence Dosimetry* (Elsevier, Amsterdam, 2003).
[20]S. W. S. McKeever, "Optically stimulated luminescence dosimetry," Nucl. Instrum. Methods Phys. Res. B **184**, 29–54 (2001).
[21]A. J. J. Bos, "High sensitivity thermoluminescence dosimetry," Nucl. Instrum. Methods Phys. Res. B **184**, 3–28 (2001).
[22]L. Bøtter–Jensen *et al.*, "Al_2O_3:C as a sensitive OSL dosemeter for rapid assessment of environmental photon dose rates," Radiat. Meas. **27**, 295–298 (1997).
[23]E. G. Yukihara and S. W. S. McKeever, "Spectroscopy and optically stimulated luminescence of Al_2O_3:C using time-resolved measurements," J. Appl. Phys. **100**, 083512 (2006).
[24]S. L. Meeks *et al.*, "In vivo determination of extra-target doses received from serial tomotherapy," Radiother. Oncol. **63**, 217–222 (2002).
[25]V. Schembri and B. J. M. Heijmen, "Optically stimulated luminescence (OSL) of carbon-doped aluminum oxide (Al_2O_3:C) for film dosimetry in radiotherapy," Med. Phys. **34**, 2113–2118 (2007).
[26]E. G. Yukihara *et al.*, "High-precision dosimetry for radiotherapy using the optically stimulated luminescence technique and thin Al_2O_3:C dosimeters," Phys. Med. Biol. **50**, 5619–5628 (2005).
[27]L. Bøtter-Jensen *et al.*, "Advances in luminescence instrument systems," Radiat. Meas. **32**, 523–528 (2000).
[28]S. C. Kappadath and R. E. Wendt III, "WE-D-L100J-09: Assessment of the radiation shielding for a busy PET/CT facility," Med. Phys. **34**, 2597 (2007).
[29]W. Feng *et al.*, "TU-FF-A4-04: Experimental confirmation of near parabolic shape of dose profile in cylindrical phantom for dual source CT," Med. Phys. **34**, 2571–2572 (2007).
[30]S. Tong *et al.*, "SU-FF-T-287: Measurement of gamma knife collimator factors using optically stimulated luminescence (OSL) dosimeter," Med. Phys. **34**, 2467–2468 (2007).
[31]M. Chan, L. Dauer, and C. Burman, "SU-FF-T-166: Dose measurement to ICD outside the treatment fields using optically stimulated luminescence," Med. Phys. **34**, 2439 (2007).
[32]J. Danzer *et al.*, "TH-C-M100E-02: Optically stimulated luminescence of aluminum oxide detectors for radiation therapy quality assurance," Med. Phys. **34**, 2628–2629 (2007).
[33]P. Jursinic, "SU-FF-T-169: Dosimetry characteristics of an optically stimulated luminescence dosimeter, OSLD, used for clinical measurements," Med. Phys. **34**, 2440 (2007).
[34]C. S. Reft, R. Runkel–Muller, and L. Myrianthopoulos, "In vivo and phantom measurements of the secondary photon and neutron doses for prostate patients undergoing 18 MV IMRT," Med. Phys. **33**, 3734–3742 (2006).
[35]M. C. Aznar, "Real-time *in vivo* luminescence dosimetry in radiotherapy and mammography using Al_2O_3:C," Ph.D. thesis, Risø National Laboratory, 2005.
[36]C. E. Andersen *et al.*, in *Standards and Codes of Practice in Medical Radiation Dosimetry* (IAEA, Vienna, 2003), 2, p. 353.
[37]C. E. Andersen *et al.*, "An algorithm for real-time dosimetry in intensity-modulated radiation therapy using the radioluminescence signal from Al_2O_3:C," Radiat. Prot. Dosim. **120**, 7–13 (2006).
[38]R. Gaza and S. W. S. McKeever, "Near-real-time radiotherapy dosimetry using optically stimulated luminescence of Al_2O_3:C: Mathematical models and preliminary results," Med. Phys. **32**, 1094–1102 (2005).
[39]R. Gaza, "A fiber-optics, real-time dosimeter based on optically stimulated luminescence of Al_2O_3:C and KBr:Eu, for potential use in the radiotherapy of cancer," Ph.D. thesis, Oklahoma State University, 2004.
[40]J. C. Polf, "A study of optically stimulated luminescence in Al_2O_3 fibers for the development of a real-time, fiber optic dosimetry system," Ph.D. thesis, Oklahoma State University, 2002.
[41]J. C. Polf *et al.*, "Real-Time luminescence from Al_2O_3 fiber dosimeters," Radiat. Meas. **38**, 227–240 (2004).
[42]P. R. Almond *et al.*, "AAPM's TG-51 protocol for clinical reference dosimetry of high-energy photon and electron beams," Med. Phys. **26**, 1847–1870 (1999).
[43]International Organization for Standardization, Guide to the expression of uncertainty in measurement (International Organization for Standardization, Switzerland, 1995).
[44]E. G. Yukihara *et al.*, "Effect of high-dose irradiation on the optically stimulated luminescence of Al_2O_3:C," Radiat. Meas. **38**, 317–330 (2004).
[45]C. J. Marckmann *et al.*, "Optical fibre dosemeter systems for clinical applications based on radioluminescence and optically stimulated luminescence from Al_2O_3:C," Radiat. Prot. Dosim. **120**, 28–32 (2006).
[46]J. M. Edmund and C. E. Andersen, "Temperature dependence of the Al_2O_3:C response in medical luminescence dosimetry," Radiat. Meas. **42**, 177–189 (2007).
[47]P. Mobit, E. Agyingi, and G. Sandison, "Comparison of the energy-response factor of LiF and Al_2O_3 in radiotherapy beams," Radiat. Prot. Dosim. **119**, 497–499 (2006).
[48]R. C. Tailor *et al.*, "Consistency of absorbed dose to water measurements using 21 ion-chamber models following the AAPM TG51 and TG21 calibration protocols," Med. Phys. **33**, 1818–1828 (2006).
[49]R. C. Tailor and W. F. Hanson, "Calculated absorbed-dose ratios, TG51/TG21, for most widely used cylindrical and parallel-plate ion chambers over a range of photon and electron energies," Med. Phys. **29**, 1464–1472 (2002).
[50]M. S. Huq, "Comment on "Calculated absorbed-dose ratios, TG51/TG21, for most widely used cylindrical and parallel-plate ion chambers over a range of photon and electron energies" [Med. Phys. **29**, 1464–1472 (2002)]," Med. Phys. **30**, 473–477 (2003).